International Journal of Mechanical, Industrial and Aerospace Sciences
ISSN: 2517-9950
Vol:8, No:6, 2014

CFD Modeling of Insect Flight at Low Reynolds Number

Wu Di, Yeo Khoon Seng, Lim Tee Tai

***Abstract*—**The typical insects employ a flapping-wing mode of flight. The numerical simulations on free flight of a model fruit fly (Re=143) including hovering and are presented in this paper. Unsteady aerodynamics around a flapping insect is studied by solving the three-dimensional Newtonian dynamics of the flyer coupled with Navier-Stokes equations. A hybrid-grid scheme (Generalized Finite Difference Method) that combines great geometry flexibility and accuracy of moving boundary definition is employed for obtaining flow dynamics. The results show good points of agreement and consistency with the outcomes and analyses of other researchers, which validate the computational model and demonstrate the feasibility of this computational approach on analyzing fluid phenomena in insect flight. The present modeling approach also offers a promising route of investigation that could complement as well as overcome some of the limitations of physical experiments in the study of free flight aerodynamics of insects. The results are potentially useful for the design of biomimetic flapping-wing flyers.

***Keywords*—**Free hovering flight, flapping wings, fruit fly, insect aerodynamics, leading edge vortex (LEV), computational fluid dynamics (CFD), Navier-Stokes equations (N-S), fluid structure interaction (FSI), generalized finite-difference method (GFD).

I. Introduction

WITH the advent in the progressive research for the applications and fabrication of autonomous micro aerial vehicles (MAV) or unmanned air vehicles (UAV), flapping mode flight is largely and widely studied in the past few years. With a wing spanwise of less than 10cm and a flight speed a few meters per second, MAVs experience the same low Reynolds number ($10^0 - 10^5$) flight conditions as their biological counterparts. In this flow regime, flapping wings type flight gains more efficiency, maneuverability and a wide range of speed over the rigid fixed wings mode, which might be the reason of its presence in nature among millions of species of birds and insects. However, researchers have long realized the "quasi-steady" aerodynamics assumption is unable to capture the physical phenomena or forces generation in flapping flight properly at this scale where the unsteady state flow mechanism dominates. In the past few decades, much work has been done to study the aerodynamics and energetics of insect flight and considerable progress has been made in these areas. The studies of Ellington [1]-[6], Dickinson [7], Ellington et al. [8], Dickinson et al. [9], Sane and Dickinson [10], Birch and Dickinson [11] and others revealed unsteady fluid mechanism in experimental aspects. Computer-based studies have also begun to play a bigger role in recent years to help unravel the intricacies of insect flight, most notably through the works of Liu et al. [12], Wang [13], Ramamurti and Sandberg [14], Sun and Tang [15] and Aono et al. [16]. These efforts have been successful in identifying and clarifying the high lift mechanisms available to flapping-wing insects to overcome weight.

Few works have focused on numerically studying the unsteady flows around 3D free flapping flyer, largely owing to difficulties in modeling the complicated geometry and in simulating the 3D movements of wings. Additionally, the kinematics and kinetics are inferred from observations of subjects, whose behavior it can be very difficult to control. As consequences, the measurements obtained from tethered insect may not truly reflect conditions in free flight. In this paper, we present a computational study on the low Reynolds number flight of a model fruit fly. The numerical model integrates the computational fluid dynamics of the flow with the three-dimensional Newtonian dynamics of the flyer and the governing Navier-Stokes equations. In contrast to the other computational studies, the wing kinematics employed in this work is not acquired from published experimental data. Instead, a basic set of sinusoidal wing kinematics are provided and allowed to evolve in time to achieve designated hovering flight with small deviations. Stroke plane adjustment and mean positional angle shifting are employed to regulate airspeed and stabilize the body pitch angle, respectively. Visualization of flow field around the model fruit fly in flight has also been obtained.

Wu Di, Research Fellow, is with the Department of Mechanical Engineering, National University of Singapore, 9 Engineering Drive 1, Singapore 117576 (e-mail: mpewudi@nus.edu.sg).

Yeo Khoon Seng. Associate Professor, is with the Department of Mechanical Engineering, National University of Singapore, 9 Engineering Drive 1, Singapore 117576(phone: +65-6516-2246; fax: +65-67791459; e-mail: mpeyeoks@nus.edu.sg).

Lim Tee Tai, Professor, is with the Department of Mechanical Engineering, National University of Singapore, 9 Engineering Drive 1, Singapore 117576, (e-mail: mpelimtt@nus.edu.sg).

II. Materials and Methods

A. Morphological and Kinematic Model

For the present work, we have adopted the morphological data on fruit fly *Drosophila melanogaster* from Fry et al. [17] for our computer model of a low-Re flapping wing flyer. The geometric model of the flyer itself was constructed from photographic images of the insect. The model flyer, referred to here as the *model insect*, has a body length of 2.78 mm and wing length $R = 2.39mm$. The wings are assumed to be rigid and of uniform thickness equal to 2% of wing length. Considering that the aerodynamic influence of the wing root is likely to be negligible, we did not model the wing base for simplicity, but instead curtailed the wings at a short distance

from the body.

According to measured data in [17], the weight of insect is $W = 0.96mg$, wing mean chord $\bar{c} = 0.874mm$, stroke angle $\Phi = 2.44rad.$ (140°) and average wing flapping frequency $f = 218Hz$. The Reynolds number in the hovering flight can be defined as

$$\mathrm{Re} = \frac{\bar{c} \cdot U_{ref}}{\nu} = \frac{R \cdot 2\Phi \cdot f \cdot \bar{c}}{\nu} = \frac{4R^2 \cdot \Phi \cdot f}{\nu \cdot AR} \quad (1)$$

where ν is the kinematic viscosity of air ($1.5 \times 10^{-5} m^2 s^{-1}$), U_{ref} the average flapping velocity of the wing tip and aspect ratio $AR = (2R)^2 / S$ with the surface area of a wing pair $S = 2R\bar{c}$. The Reynolds number Re thus works out to be nominally around 143.

B. Fluid Dynamics Modeling

The dynamics of the fluid is governed by the incompressible non-dimensional Navier-Stokes (NS) equations, given in the arbitrary Lagrangian-Eulerian (ALE) form:

$$\nabla \cdot u = 0 \quad (2)$$

$$\partial_t u = -(u - u^g) \cdot \nabla u + \frac{1}{\mathrm{Re}} \Delta u - \nabla p \quad (3)$$

where $u(x,t)$ and $p(x,t)$ ($x \in \Omega(t)$)represent the velocity and pressure fields of the fluid domain $\Omega(t)$, respectively. The u^g is the convection velocity of the computational node, which is equal to zero for stationary nodes. The above equations are solved on a hybrid Cartesian cum meshfree grid system, wherein immersed bodies/boundaries and their near fluid neighborhoods are discretized by meshfree nodes. The meshfree nodes convect with the motion of bodies/boundaries. Fig. 1 shows the nodal system on the model insect generated using an available finite-element grid generator. The flyer is located in a cubic domain with boundaries set at a distance of about 8 wing-lengths away flyer. The cubic domain is discretized by a 221^3 Cartesian grid system (See Fig. 2). The grid is non-uniform with coarse grid on the outside and fine grid near the center where the model insect is located to give good resolution to the immediate flow around the flyer. The final grid has been selected through trials and comparison with experiments to ensure well-converged numerical performance.

Solution by the present hybrid-grid scheme utilizes a projection-based method, which has been described by Chew et al. [18] and Yu et al. [19], and will not be elaborated here. The hybrid grid combines great geometry flexibility and accuracy of boundary definition with the computational efficiency of a Cartesian background grid used in bulk of the flow domain. The cloud of meshfree nodes employed around the model also gives good resolution to the fluid boundary layer. In the present case, the meshfree nodes constitute around 1% of the total nodal population. The Cartesian background grid/nodes are stationary in space in most applications, but they can also be convected with the overall motion of the model flyer if necessary. The latter is particularly useful in problems where the flyer is allowed to traverse freely through space, such as in forward or backward flight.

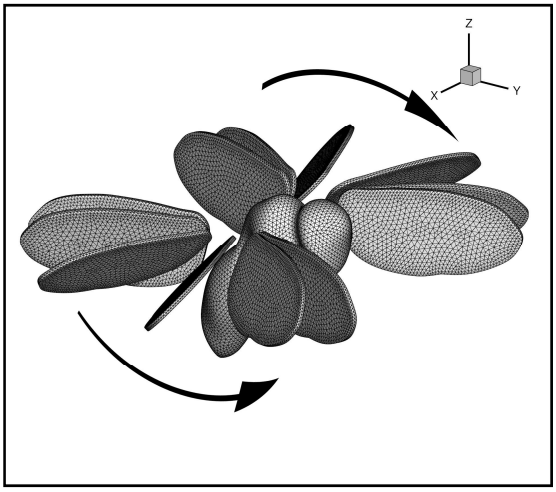

Fig. 1 Discretized fruit fly model in downstroke flapping

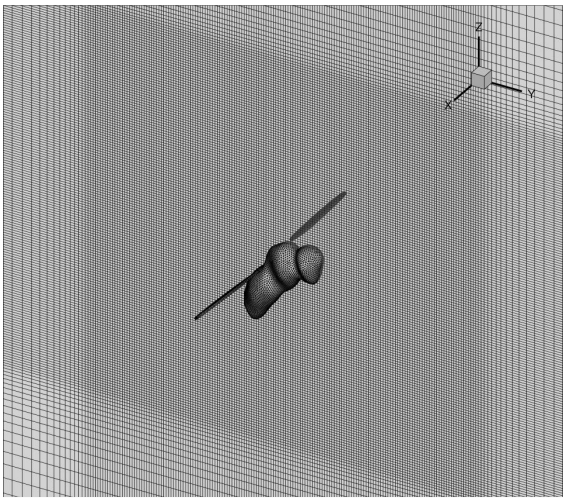

Fig. 2 Comparison between the messless points and its background Cartesian mesh

C. Fluid-Body Interaction

The flapping wing action of the model flyer drives the flow, whose dynamics has been stated above. The reaction force of the fluid in turn motivates the motion of the flyer in accordance with Newton's laws. Let $V_C(t)$ and $\omega(t)$ denote the linear and angular velocities of the flyer of mass *M* at its center of mass *C*, respectively. The governing dynamical equations for the flyer are then given by:

$$\left.\begin{aligned}
\frac{dX_C(t)}{dt} &= V_C(t) \\
\frac{d\Theta(t)}{dt} &= [K(t)]\cdot\omega(t) \\
\frac{d(M\cdot V_C(t))}{dt} &= -Mg\cdot i_z + \int_{\Gamma(t)} [\sigma]\cdot n\, d\Gamma \\
\frac{d([I(t)]\cdot\omega(t))}{dt} &= \int_{\Gamma(t)} (x - X_C(t))\times([\sigma]\cdot n)\, d\Gamma
\end{aligned}\right\} \quad (4)$$

where $\Theta(t)$ is a rotation angle vector and $[K(t)]$ a transformation matrix. $[I(t)]$ is the inertia tensor of the flyer, while $[\sigma]$ is the Newtonian fluid stress tensor. The velocity of nodes on the moving body and wings of the model flyer is given by

$$u(x,t) = V_C(t) + V_{x/C}(t) + \omega(t)\times(x - X_C(t)) \quad (5)$$

where $V_{x/C}(t)$ represents the velocity of nodes relative to the body frame of flyer, which is non-zero for nodes of the wings.

As can be seen, both equations of fluid (2), (3) and model flyer (4), (5) require information about the surface (body and wing) configuration $\Gamma(t)$ of the flyer. The time-dependent surface configuration $\Gamma(t, X_C(t), \Theta(t))$ comprises information about the current disposition of the flyer in its body frame, which is known, as well as information on the current spatial location $X_C(t)$ and orientation $\Theta(t)$ of the flyer, which are unknown. The solution of the fluid-body interaction problem at time *t* thus involves solving the coupled equations of the fluid and the flyer, given above, while simultaneously iterating on $X_C(t)$ and $\Theta(t)$ to determine the configuration $\Gamma(t, X_C(t), \Theta(t))$ that satisfies all the governing equations and conditions (2) to (5). This is essentially a fixed-point iteration problem, which could be symbolically represented by the following process equation:

$$\Gamma(t) = S(F(\Gamma(t))), \quad (6)$$

where *F* symbolically denotes the flow solver, which computes the force/moment loading on the currently estimated configuration $\Gamma(t)$, and *S* is the body dynamic solver, which computes an updated configuration $\Gamma(t)$ of the flyer. This process of estimation and update is repeated until the change between consecutive estimates of $\Gamma(t)$ is less than a prescribed small real number ε, the convergence criterion. The free flight of the model insect is then described by the solution of $\Gamma(t)$ as a function of time. The above methodology has been described in some detail and validated in fluid-body interaction study by Yu et al. [19].

III. Results and Discussion

Fig. 3 shows the free normal hovering dynamics of the model fruit fly over a period of 40 wing cycles. The *y*-component of displacement fluctuation is the largest (Fig. 3A), while pitching is the largest component of rotational fluctuation (Fig. 3B), both within individual wing cycles and over the course of hovering simulation. Over the course of the 40 wing cycles, the body deviates<4% of a wing length from the designed hovering position (Fig. 3A), while the pitching angle of the body $\chi(t)$ oscillates within a narrow band of < 3° after the 10th cycle (Fig. 3B). In fact, both displacement and pitching oscillations decrease with increasing wing cycles, showing a gradual convergence towards a sustained quasi-steady hovering state. The larger body fluctuations registered at the beginning is due to the flyer being initiated into flight at time *t*=0 from a rest state.

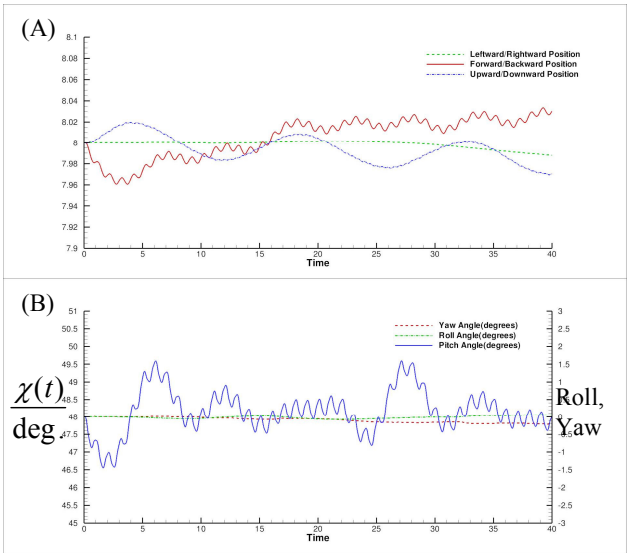

Fig. 3 (A) Translational fluctuation of the center of mass of flyer about the designated mean position. (B) Fluctuations of body orientation – mean body pitch angle $\overline{\chi} \approx 48°$ from the horizontal

Unsteady fluid flow over flapping wings is governed by the dynamics of strong vortices generated at the edges of the wings. The vortical flow over the wings of the model fruit fly comprises a leading-edge vortex (LEV) over the straight anterior margin of the wing, a wing-tip vortex (WTV) and a trailing-edge vortex (TEV). The term WTV is used here to distinguish the strong vortex that extends contiguously from the LEV over the curved section of leading edge in the distal 40% of the wing (see Fig. 4).

Fig.5 shows the vortex generation and shedding processes in hovering flight. The associated velocity fields in a lateral plane cutting across the vortex system at the wing root are also given. The bulk of vortical flow is shed via the WTV and TEV from each wing in a fairly continuous fashion during a stroke in an arc about the body. These vortices generated are roughly symmetric and of equal magnitude in the upstroke and

downstroke during normal hovering, where the stroke plane is nearly horizontal. One may also observe the jets of flow passing between the WTV and the TEV. A stacked sequence of these vortices about each wing drives the flow below the wing.

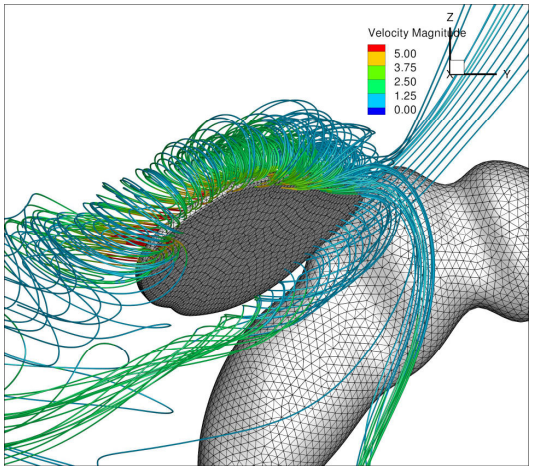

Fig. 4 Three-dimensional stream traces around the leading edge and wing tip regions

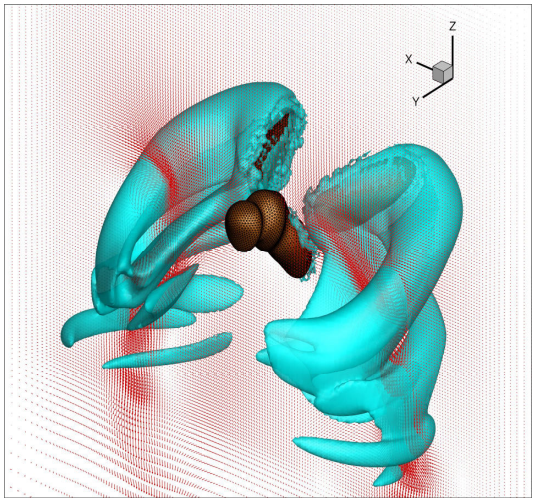

Fig. 5 Iso-vorticity surfaces around the model fruit fly during normal hovering. Also given is the velocity field in a lateral plane cutting across the vortex system

IV. Conclusions

This paper is concerned with a numerical study on the free hovering of a low Reynolds number flapping-wing flyer, modeled after the fruit fly. The unsteady flow is modeled by the incompressible Navier-Stokes equations, while the dynamics of the flyer is governed by Newton's laws of free body in a gravity field. The deviation of center of mass of the insect from the designated hovering position is typically less than 4% of one wing length while the orientation or pitching angle of the body varies within a band of less than 3 degrees for hovering flight. Flow field study shows that the flow jets induced by the wings are broadly similar to those in published results for normal hovering. The present modeling approach offers a promising route of investigation that could complement as well as overcome some of the limitations of experiments in the area of free flight aerodynamics of insects.

Acknowledgment

The generous financial support for the present work under the research grant TDSI/09-007/1A from the TDSI (National University of Singapore) is gratefully acknowledged.

References

[1] Ellington, C. P.. The aerodynamics of hovering insect flight. I. The quasi-steady analysis. *Phil. Trans. R. Soc. Lond. B* 1984; 305: 1-15.
[2] Ellington, C. P.. The aerodynamics of hovering insect flight. II.Morphological parameters. *Phil. Trans. R. Soc. Lond. B* 1984; 305: 17-40.
[3] Ellington, C. P.. The aerodynamics of hovering insect flight. III. Kinematics. *Phil. Trans. R. Soc. Lond. B* 1984; 305: 41-78.
[4] Ellington, C. P.. The aerodynamics of hovering insect flight. IV. Aerodynamic mechanisms. *Phil. Trans. R. Soc. Lond. B* 1984; 305: 79-113.
[5] Ellington, C. P.. The aerodynamics of hovering insect flight. V. A vortex theory. *Phil. Trans. R. Soc. Lond. B* 1984; 305: 115-144.
[6] Ellington, C. P.. The aerodynamics of hovering insect flight. VI. Lift and power requirements. *Phil. Trans. R. Soc. Lond. B* 1984; 305: 145-181.
[7] Dickinson, M. H.. The effects of wing rotation on unsteady aerodynamic performance at low Reynolds numbers. *J. Exp. Biol.* 1994; 192: 179-206.
[8] Ellington C. P., van den Berg, C., Willmott A. P. and Thomas A. L. R.. Leading-edge vortices in insect flight. *Nature*1996; 384: 626-630.
[9] Dickinson, M. H., Lehmann, F.-O. and Sane, S. P.. Wing rotation and the aerodynamic basis of insect flight. *Science* 1999; 284: 1954–1960.
[10] Sane S.P. and Dickinson M.H.. The control of flight force by a flapping wing: lift and drag production. *J. Exp. Biol.* 2001; 204: 2607-2626.
[11] Birch J.M. and Dickinson M.H.. The influence of wing-wake interactions on the production of aerodynamic forces in flapping flight. *J. Exp. Biol.* 2003; 206: 2257-2272.
[12] Liu, H., Ellington, C. P., Kawachi, K., Van den Berg, C. and Willmott, A. P.. A computational fluid dynamic study of hawkmoth hovering. *J. Exp. Biol.* 1998; 201: 461-477.
[13] Wang, Z. J..Two dimensional mechanism for insect hovering. *Phys. Rev. Lett.* 2000; 85: 2216-2219.
[14] Ramamurti, R. and Sandberg, W. C.. A three-dimensional computational study of the aerodynamic mechanisms of insect flight. *J. Exp.Biol.* 2002;205: 1507-1518.
[15] Sun, M. and Tang, J.. Unsteady aerodynamic force generation by a model fruit fly wing in flapping motion. *J. Exp. Biol.* 2002; 205: 55-70.
[16] Aono H., Liang F. and Liu H.. Near- and far-field aerodynamics in insect hovering flight: an integrated computational study. *J. Exp. Biol.* 2008; 211: 239-257.
[17] Fry S. N., Sayaman R. and Dickinson, M. H.. The aerodynamics of hovering flight in Drosophila. *J. Exp. Biol.* 2005; 208: 2303-2318.
[18] Chew C.S., Yeo K.S. and Shu C.. A generalized finite-difference (GFD) ALE scheme for incompressible flows around moving solid bodies on hybrid meshfree-Cartesian grids. *J. Comput. Phys.* 2006; 218: 510-548.
[19] Yu, P., Yeo, K.S., ShyamSundar, D. and Ang, S.J.. A three-dimensional hybrid meshfree-Cartesian scheme for fluid–body interaction.*Int. J. Numer. Meth. Engng.* 2011; 88: 385–408.